

ORIGINAL RESEARCH COMMUNICATION

Regulation of Calcium Fluxes by GPX8, a Type-II Transmembrane Peroxidase Enriched at the Mitochondria-Associated Endoplasmic Reticulum Membrane

Edgar Djaha Yoboue,^{1,*} Alessandro Rimessi,^{2,*} Tiziana Anelli,^{1,3} Paolo Pinton,² and Roberto Sitia^{1,3}

Abstract

Glutathione peroxidases (GPXs) are enzymes that are present in almost all organisms with the primary function of limiting peroxide accumulation. In mammals, two of the eight members (GPX7 and GPX8) reside in the endoplasmic reticulum (ER). A peculiar feature of GPX8 is the concomitant presence of a conserved N-terminal transmembrane domain (TMD) and a C-terminal KDEL-like motif for ER localization.

Aims: Investigating whether and how GPX8 impacts Ca^{2+} homeostasis and signaling.

Results: We show that GPX8 is enriched in mitochondria-associated membranes and regulates Ca^{2+} storage and fluxes. Its levels correlate with $[\text{Ca}^{2+}]_{\text{ER}}$, and cytosolic and mitochondrial Ca^{2+} fluxes. GPX7, which lacks a TMD, does not share these properties. Deleting or replacing the GPX8 TMD with an unrelated N-terminal membrane integration sequence abolishes all effects on Ca^{2+} fluxes, whereas appending the GPX8 TMD to GPX7 transfers the Ca^{2+} -regulating properties.

Innovation and Conclusion: The notion that the TMD of GPX8, in addition to its enzymatic activity, is essential for regulating Ca^{2+} dynamics reveals a novel level of integration between redox-related proteins and Ca^{2+} signaling/homeostasis. *Antioxid. Redox Signal.* 27, 583–595.

Keywords: endoplasmic reticulum, mitochondria associated membrane (MAM), calcium (Ca^{2+}) signaling, glutathione peroxidases, membrane topology

Introduction

THE ENDOPLASMIC RETICULUM (ER) is a multifunctional organelle in which about one-third of the proteome folds and undergoes key post-translational modifications, such as *N*-glycosylation and disulfide bond formation. This network of tubules and cisternae is also involved in redox homeostasis, membrane lipid synthesis, and Ca^{2+} storage and signaling (8, 18, 20). The ER establishes close contacts with the plasma membrane and other organelles, such as mitochondria (28). In the past few years, the so-called mitochondria-associated membranes (MAM) emerged as key integration hubs for Ca^{2+} , lipid metabolism, and redox signaling homeostasis.

Innovation

The interplays between redox and Ca^{2+} homeostasis/signaling and the dynamics of inter-organelle communication are of fundamental importance in cell pathophysiology. The involvement of endoplasmic reticulum (ER)-residing peroxidases in these expanding research fields was still unexplored. Our study identifies GPX8 as a novel important integrator of redox and Ca^{2+} signals at the mitochondria-ER interface and uncovers a critical role for its conserved transmembrane region in the regulation of Ca^{2+} dynamics.

¹Protein Transport and Secretion Unit, Division of Genetics and Cell Biology, IRCCS Ospedale San Raffaele, Milan, Italy.

²Section of Pathology, Oncology and Experimental Biology, Laboratory for Technologies of Advanced Therapies (LTTA), Department of Morphology, Surgery and Experimental Medicine, University of Ferrara, Ferrara, Italy.

³Vita-Salute San Raffaele University, School of Medicine, Milan, Italy.

*These authors contributed equally to this work.

MAM are subregions of the ER resulting from the close contact between the ER and mitochondria. MAM are enriched in some Ca^{2+} -handling proteins such as inositol 1,4,5-triphosphate receptors (IP3Rs), which release Ca^{2+} from the ER toward mitochondria and the cytosol and for diverse physiological purposes (13, 15, 32, 35, 42, 43). Sarcoendoplasmic reticulum ATPase (SERCA) that guarantees prompt ER Ca^{2+} replenishment is also, in part, located in MAM (11, 27). Moreover, it emerges that MAM also contain ER proteins that are primarily known for their involvement in protein folding and redox regulation (3, 24). Thus, we previously showed that Ero1 α , a flavoprotein that generates H_2O_2 while promoting disulfide bond formation, is enriched in MAM and regulates the ER Ca^{2+} storage and mitochondrial Ca^{2+} fluxes (1).

H_2O_2 is a double-edged sword for cells, acting as an essential second messenger but becoming harmful if in excess (16, 34). To limit its toxicity, H_2O_2 produced during Ero1-dependent oxidative folding has to be cleared by luminal peroxidases (8). Glutathione peroxidase 8 (GPX8) is a type II transmembrane protein with rare, peculiar structural features. Indeed, in addition to a highly conserved N-terminal transmembrane domain (TMD), GPX8 harbors a C-terminal KEDL ER localization motif (23, 39). GPX8 was shown to limit ER hyperoxidation and H_2O_2 leakage to the cytosol in conditions of deregulated Ero1 α activity (30). Furthermore, GPX8 is believed to form heterotrimeric complexes with Ero1 α and protein disulfide isomerase (PDI), thus coupling clearance of H_2O_2 with disulfide bond formation (31). Similar to Ero1 α , GPX8 expression is induced by hypoxia (5).

Considering the apparent synergies between Ero1 α and GPX8 and the Ca^{2+} -regulatory roles of the former, we set out to investigate the involvement of GPX8 in Ca^{2+} homeostasis and signaling.

The experiments described here show that GPX8 is enriched in MAM and regulates Ca^{2+} signaling. We also demonstrate that its TMD is essential for the regulation of Ca^{2+} fluxes. Our data reveal a new player involved in the regulation of the physiological important Ca^{2+} dynamics and unveil the molecular features required for these regulatory functions.

Results

GPX8 is enriched in MAM in HeLa cells

First, we assessed the subcellular localization of GPX8 by fractionation assay that allows the separation of ER, mitochondria, and MAM (46). Analysis of the different fractions revealed that GPX8, co-fractionates with other MAM markers such as IP3R3 and ASCL4 (Fig. 1). Instead, the chaperone GRP94 was mainly enriched in the ER fraction. Thus, endogenous GPX8 accumulates in MAM in standard conditions.

GPX8 level modulates Ca^{2+} dynamics

Considering the strong enrichment of GPX8 in MAM, a key hub for Ca^{2+} signaling, we assessed the consequences of its overexpression (Fig. 2A; Supplementary Fig. S1A; Supplementary Data are available online at www.liebertpub.com/ars) or silencing (Fig. 2B; Supplementary Fig. S1B) on intracellular Ca^{2+} dynamics. We first monitored the levels of Ca^{2+} in the ER ($[\text{Ca}^{2+}]_{\text{ER}}$) and histamine-induced IP3-dependent release toward the mitochondria and the cytosol, which are crucial signaling processes. To this end, we used

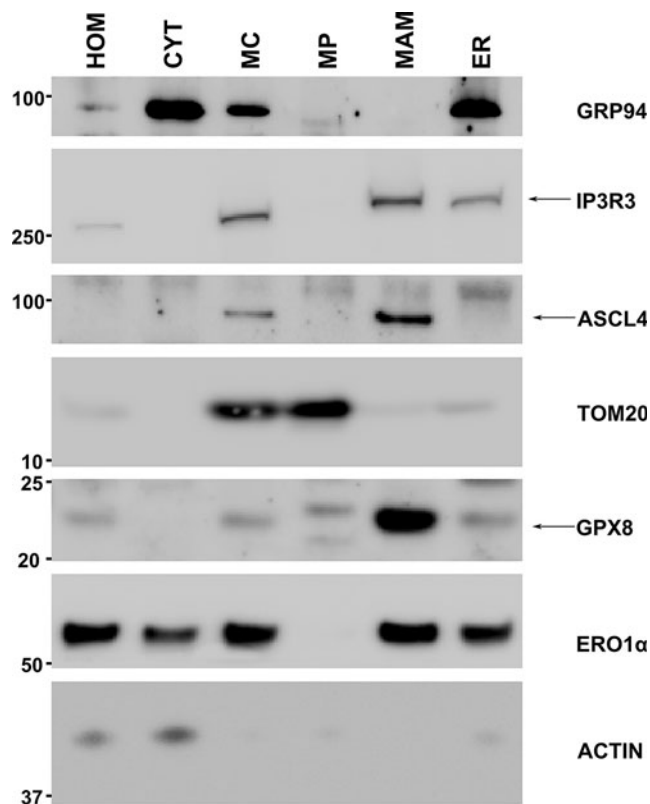


FIG. 1. Endogenous GPX8 is highly enriched in MAM in HeLa cells. HeLa cells homogenates (Hom) were fractionated by sequential centrifugation to obtain cytosol (Cyt), crude mitochondria (MC), pure mitochondria (MP), MAM, and ER fractions. Equal amounts of proteins (10 μg) from each fraction were resolved by reducing SDS-PAGE and analyzed by Western blot using the indicated antibodies. Note the enrichment of GPX8 in MAM. Numbers on the left indicate the relative molecular weight based on co-migrating pre-stained molecular-weight markers. (See Supplementary Fig. S9 for uncropped Western blots.) ER, endoplasmic reticulum; GPX, glutathione peroxidase; MAM, mitochondria-associated membranes.

the well-known luminescent protein probe aequorin targeted to different subcellular compartments (4).

Cells overexpressing GPX8 displayed a significantly lower $[\text{Ca}^{2+}]_{\text{ER}}$ at steady state (Fig. 2A, left panel), as also confirmed in a single-cell assay using the high Ca^{2+} -sensitive FRET-based DIER probe (Supplementary Fig. S2). Addition of the agonist histamine induces IP3 elevation, allowing the IP3R-dependent Ca^{2+} release from the ER toward the mitochondria and the cytosol. GPX8 overexpression strongly reduced these IP3-dependent Ca^{2+} fluxes (Fig. 2A, middle panels). The ER Ca^{2+} -release rate was also strongly reduced, suggesting that the lower mitochondrial and cytosolic responses were consequences of an impaired capacity of the ER to release Ca^{2+} in response to agonist stimulation.

Using the high-affinity Ca^{2+} -probe FURA2-AM, we then investigated whether GPX8 level could alter the Ca^{2+} release induced by an oxidative stimulus such as H_2O_2 that triggers a progressive Ca^{2+} release by IP3Rs independently of IP3 elevation (14). In cells overexpressing GPX8, the increase in $[\text{Ca}^{2+}]_{\text{cyto}}$ evoked by H_2O_2 was also reduced (Supplementary Fig. S3). GPX8 silencing had opposite effects, increasing

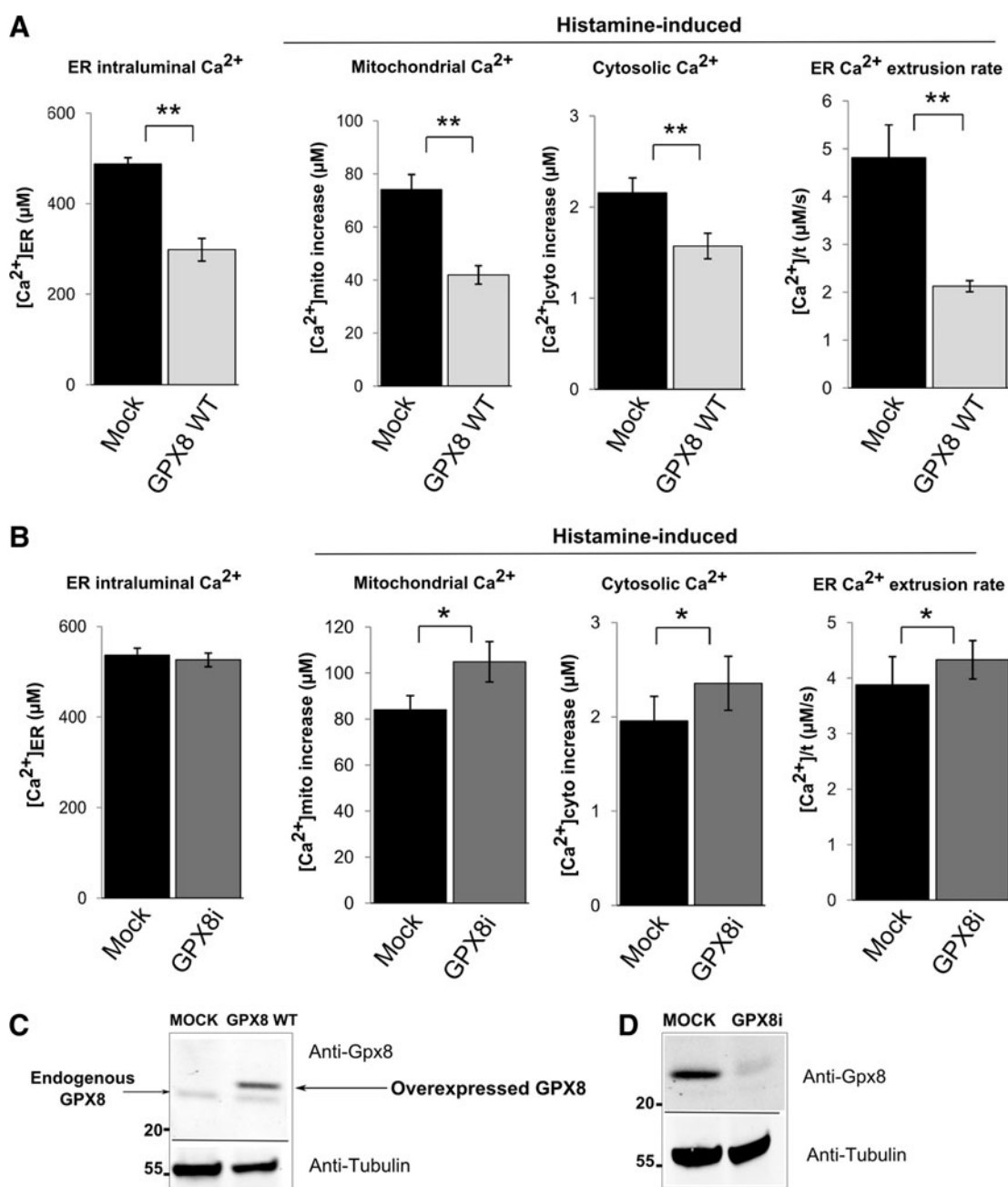


FIG. 2. GPX8 level modulates ER Ca^{2+} concentration and fluxes. (A) To monitor the effects of GPX overexpression on Ca^{2+} fluxes, HeLa cells were co-transfected with plasmids driving the expression of ER-, mitochondria- or cytosol-targeted aequorin probes, and an HA-tagged GPX8 (GPX8 WT) or an empty parental vector as a control (mock). After 36 h of transfection, the indicated parameters were analyzed as described in the Materials and Methods section. The data are pooled from ~20 independent experiments and are expressed as the means \pm SE, $**p < 0.01$. (B) To downregulate GPX8, HeLa cells expressing suitable aequorin probes (A) were transfected with an siRNA that was specific for GPX8 (GPX8i), or a negative control siRNA (mock) and analyzed after 36 h. $n = 15$ independent experiments, $*p < 0.05$. (C) and (D) are representative Western blot pictures showing GPX8 overexpression level and knockdown efficiency, respectively. (See Supplementary Fig. S10 for uncropped Western blots.) SE, standard error.

Ca^{2+} fluxes into the mitochondria and the cytosol without significantly perturbing $[\text{Ca}^{2+}]_{\text{ER}}$ (Fig. 2B). Thus, GPX8 plays a role in regulation of Ca^{2+} dynamics.

GPX8 level modulates both SERCA2b activity and ER Ca^{2+} leakage

We focused next on the observation that GPX8 overexpression decreases the $[\text{Ca}^{2+}]_{\text{ER}}$ at steady state. This pa-

rameter depends on the balance between ER refilling that is mediated mainly by SERCA and passive leak through IP3Rs and/or translocon components (25, 37, 41, 44). Thus, we used Ca^{2+} refilling assays to compare SERCA activity in cells overexpressing GPX8 and control cells. The activity of SERCA2b, the isoform expressed in HeLa cells, was slower in cells overexpressing GPX8 (Fig. 3A, left panel). Moreover, passive Ca^{2+} efflux (*i.e.*, leakage) from the ER was slightly increased by GPX8 overexpression, as determined by

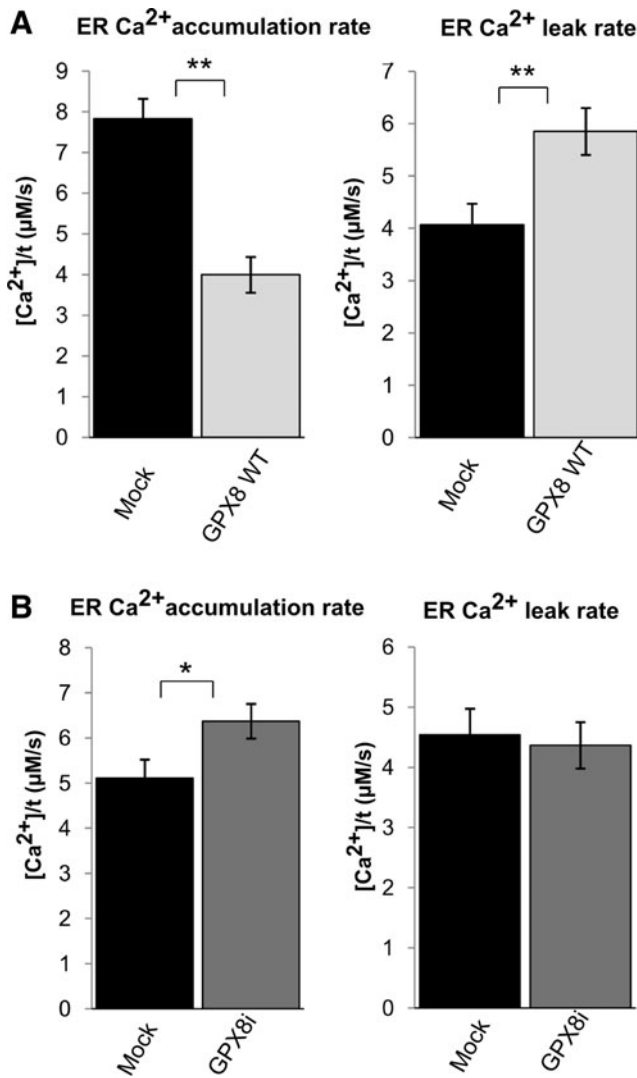


FIG. 3. GPX8 level modulates the SERCA2b activity and ER Ca²⁺ leakage. HeLa cells overexpressing GPX8 (A) or treated with GPX8 siRNA (B) were analyzed as described in Fig. 2, and the rates of ER Ca²⁺ refilling and the passive leak were measured as described in the Materials and Methods section. The data are pooled from ~20 independent experiments and are expressed as the mean ± SE, ***p* < 0.01 and **p* < 0.05.

treatment with the SERCA inhibitor tBHQ (Fig. 3A, right panel). Instead, GPX8 silencing increased the ER Ca²⁺ entry rate (Fig. 3B) without significant effects on Ca²⁺ leakage.

Thus, GPX8 levels modulate [Ca²⁺]_{ER} mainly through SERCA activity and partially by influencing passive Ca²⁺ leakage.

The TMD of GPX8 is essential but not sufficient for regulating Ca²⁺ signaling

Next, we asked whether the peculiar GPX8 topology was important for its activity in Ca²⁺ regulation. GPX8 is a type II membrane protein, with an 18-amino-acid N-terminal cytosolic peptide, a hydrophobic stretch predicted to span the membrane (TMD), and the catalytic region in the ER lumen.

The presence of a TMD is intriguing, considering that GPX8 has a C-terminal KEDL motif that mediates its retrieval to the ER (33).

We generated a construct named S-GPX8, by substituting the GPX8 TMD with the cleavable ER signal peptide of the protein ERp44 (Fig. 4A). Immunoblot and imaging assays confirmed that S-GPX8 is correctly expressed and localized in the ER (Fig. 4B, C). Thus, the TMD is not mandatory for GPX8 ER retention. However, S-GPX8 had no effects on Ca²⁺ fluxes. Cells overexpressing it displayed a [Ca²⁺]_{ER} and mitochondrial and cytosolic Ca²⁺ responses similar to mock-transfected cells (Fig. 5A). In good accordance with our previous conclusions, overexpression of S-GPX8 had also no discernible effects on ER Ca²⁺ uptake or leakage (Fig. 5B). Thus, the TMD is essential for the GPX8 effects on Ca²⁺ homeostasis.

To determine the intrinsic role of the GPX8 TMD, we fused the GPX8 N-terminus to an irrelevant protein. To this end, we chose the Halo-tag (Fig. 6A, B), a recombinant protein capable of binding covalently fluorescent ligands and shown not to alter the properties of other ER proteins (19, 22). Neither TMD8-Halo nor a variant with a cleavable leader sequence (S-Halo) affected [Ca²⁺]_{ER} and release (Fig. 6C, D). Altogether, these data suggest that although the TMD of GPX8 is essential for its effects on Ca²⁺ dynamics, element(s) present in the luminal portion is (are) also required for full regulation.

Regulation of Ca²⁺ dynamics relies on both the TMD and peroxidatic cysteines of GPX8

To determine whether the peroxidatic activity of GPX8 could be required for Ca²⁺ regulation, we analyzed the effects on Ca²⁺ signaling of a GPX8 mutant in which cysteines 79 and 108, which are essential for enzymatic activity (31, 45), had been replaced with serine and alanine, respectively (GPX8-CCSA). When expressed at levels similar to WT-GPX8, the GPX8-CCSA mutant lost most of its inhibitory effect on [Ca²⁺]_{ER} and mitochondrial Ca²⁺ responses (Fig. 6E, F), suggesting that the GPX8 peroxidatic cysteines are also necessary to efficiently modulate Ca²⁺ homeostasis.

These notions were strengthened by performing a comparative analysis with GPX7 (Fig. 7). Similar to GPX8, GPX7 resides in the ER and both enzymes share significant structural similarities, except that GPX7 harbors a cleavable ER signal peptide and, hence, behaves as a soluble ER protein (23, 29, 40). GPX7 overexpression had no obvious effects on Ca²⁺ dynamics (Fig. 7D). However, a fusion protein in which the GPX7 N-terminus is substituted with the GPX8 TMD displayed similar properties to GPX8, with a reduction of [Ca²⁺]_{ER} and IP3R-dependent mitochondrial and cytosolic Ca²⁺ responses (Fig. 7). Altogether, these results indicate that an active GPX moiety needs to be bound to the membrane to control ER Ca²⁺ homeostasis.

The TMD of GPX8 is specifically required for regulation of Ca²⁺ dynamics

Next, we sought evidence to determine whether membrane insertion *per se* was sufficient for affecting Ca²⁺ dynamics, or whether information specifically contained within the conserved GPX8 TMD sequence was required. To address this question, we replaced the entire GPX8 N-terminal region or

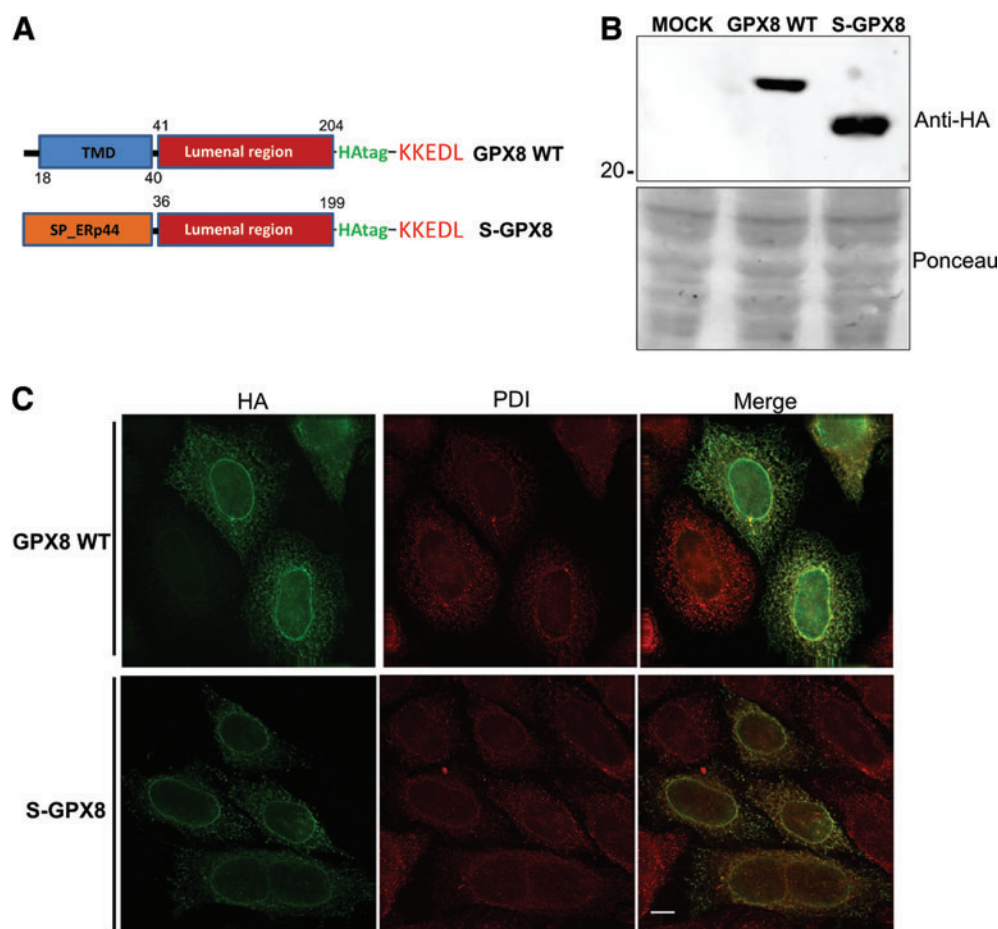


FIG. 4. The GPX8-TMD is not necessary for its expression and ER localization. (A) Diagram summarizing the key features of the GPX8 variants utilized (GPX8-WT and S-GPX8). The N-terminal 40 amino acids of GPX8, which include the TMD, were substituted by the cleavable leader peptide of the ER protein ERp44 (SP_ERp44). (B) Western blot showing that the S-GPX8 variant is correctly expressed and cleaved, compared with the WT. Ponceau red staining assessed of protein loading. Numbers on the *left* indicate the relative molecular weight based on co-migrating pre-stained molecular-weight markers. (See Supplementary Fig. S11 for uncropped Western blots.) (C) Immunofluorescence staining performed on fixed HeLa transfectants producing the GPX8 variants depicted in (A) co-stained with anti-HA (which recognizes the GPX8 transgene) and anti-PDI (used as ER marker) as antibodies. (Scale bar, 10 μ m). PDI, protein disulfide isomerase; TMD, transmembrane domain. To see this illustration in color, the reader is referred to the web version of this article at www.liebertpub.com/ars.

the sole TMD with the corresponding portions of asialoglycoprotein receptor 1 (ASGR1), a type II membrane protein involved in serum glycoprotein turnover (3b, 10, 38) (Fig. 8A).

Clearly, both ASGR-GPX8 chimeric molecules (CA-TMDA-GPX8 and C8-TMDA-GPX8) were properly expressed and ER localized, further confirming that the GPX8 N-terminal region is not necessary for ER localization (Fig. 8B, C). However, cells overexpressing CA-TMDA-GPX8 or C8-TMDA-GPX8 showed no alteration of $[Ca^{2+}]_{ER}$ and displayed IP3-dependent mitochondrial responses similar to mock transfectants (Fig. 8D). Thus, the GPX8 transmembrane stretch sequence is specifically needed for the regulation of Ca^{2+} dynamics by GPX8.

Discussion

GPXs are found in almost all kingdoms of life, playing important roles in fertility, inflammation, and cancer (6, 39).

Two of the eight mammalian family members, GPX7 and GPX8, are localized in the ER where they scavenge H_2O_2 produced by Erol α , avoiding lethal oxidative stress and further fueling disulfide bond formation *via* PDI or other resident oxidoreductases (9, 23, 29, 45). In this study, we focused on GPX8, because it the last identified family member, and it presents a peculiar topology as a type II membrane protein with a KEDL C-terminal sequence.

The first conclusion that emerges from our studies is that GPX8 is enriched in MAM (Fig. 1). This result is strengthened by independent studies showing that the NS3-4A protease of the hepatitis C virus targets MAM in human cells (17), with GPX8 being the top-hit target of the protease (21). Thus, GPX8 is a novel MAM-enriched redox protein.

We also showed that GPX8 level affects Ca^{2+} homeostasis and signaling. Cells overexpressing GPX8 have reduced $[Ca^{2+}]_{ER}$ and IP3-dependent mitochondrial and cytosolic Ca^{2+} transients, whereas its silencing had opposite effects (Fig. 2).

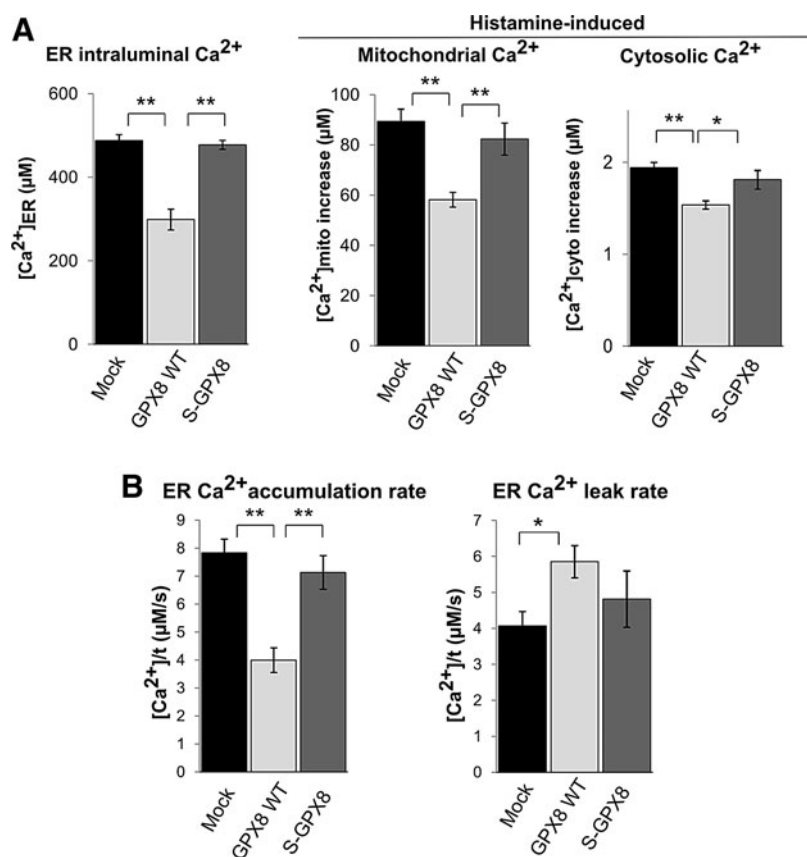


FIG. 5. The GPX8 TMD is essential for Ca²⁺ dynamics regulation. [Ca²⁺]_{ER}, mitochondrial, and cytosolic Ca²⁺ responses (**A**) and rates of ER Ca²⁺ accumulation and passive leak (**B**) were determined in the indicated HeLa transfectants. The data are pooled from ~25 independent experiments and are expressed as the means ± SE, ***p* < 0.01 and **p* < 0.05.

A third important conclusion of our work is that the TMD of GPX8 is essential for impacting Ca²⁺ homeostasis (Fig. 5). Interestingly, regulatory information is specifically contained in the GPX8 transmembrane sequence and not in the topology that it warrants, since the ASGR1 TMD could not be a surrogate (Fig. 8). In addition, overexpressing GPX7 had no effects, unless equipped with the GPX8 TMD (Fig. 7). The inactivity of GPX7, S-GPX8, and chimeric TMD8-Halo proteins excludes the possibilities that the impaired Ca²⁺ dynamics were mere consequences of overexpressing redox-related proteins. Thus, for the first time, relevance for the GPX8 TMD is revealed.

Very similar results were obtained in different cell types (Supplementary Fig. S4) and also in a condition of oxidative stimulus (Supplementary Fig. S3), suggesting a general Ca²⁺-signaling control process and underscoring the peculiar properties of GPX8.

What could be so special about the GPX8 TMD? We first considered that the GPX8 TMD could be essential for MAM targeting. However, soluble GPX8 is also enriched in the MAM fractions (Supplementary Fig. S5) whereas it is inactive on Ca²⁺ fluxes (Fig. 5). Thus, being enriched in MAM is not sufficient and an active GPX moiety must contain a peculiar amino-acid sequence, allowing its membrane insertion to affect Ca²⁺ signaling. The TMD might anchor GPX8 in a specialized place, where its level could regulate the Ca²⁺ machinery. In this regard, our results showing an impairment of the ER Ca²⁺ refilling (Figs. 3 and 5) without basal mitochondrial Ca²⁺ changes (Supplementary Fig. S6) point at SERCA as a possible target of GPX8. GPX8 overexpression

does not influence the levels of SERCA or other Ca²⁺-related channels (Supplementary Fig. S7). But, co-immunoprecipitation experiments revealed associations between GPX8 and SERCA. However, this interaction also occurs without the GPX8 TMD (Supplementary Fig. 8).

These results not only strengthen the notion of interplay between GPX8 and SERCA but also suggest more complex mechanism(s). For example, SERCA regulation could be indirect, and it could involve other molecule(s) recruited by the GPX8 TMD. Beside the latter's identities, other key questions such as how GPX8 or other ER redox proteins are localized to the MAM deserve to be investigated (3, 12).

In sum, our data identify GPX8 as a novel component of the MAM signaling hub, underlying the essential role of its TMD in influencing integration of redox and Ca²⁺-signaling processes.

Materials and Methods

Reagents, cell lines, and transfection procedures

Polyclonal anti-GPX8 antibody was a kind gift of D. Moradpour (Lausanne, CH) and is available from Adipogen (AG-25B-0028-C100). Polyclonal anti-PDI was a kind gift of I. Braakman (Utrecht, NL). Other antibodies used for the study are anti-Ero1α 2G4 (36); anti-Halo tag (G9281; Promega); anti-ASCL4, anti-TOM20, and anti-HSP60 (sc-47997, sc-11415, and sc-13115, respectively; Santa Cruz Biotechnology); anti-SERCA2 (4388S; Cell Signaling); anti-IP3R1 (AB5804; Abcam); anti-IP3R3 (610312; BD Transduction Laboratories); anti-MCU and anti-Actin (HPA016480 and

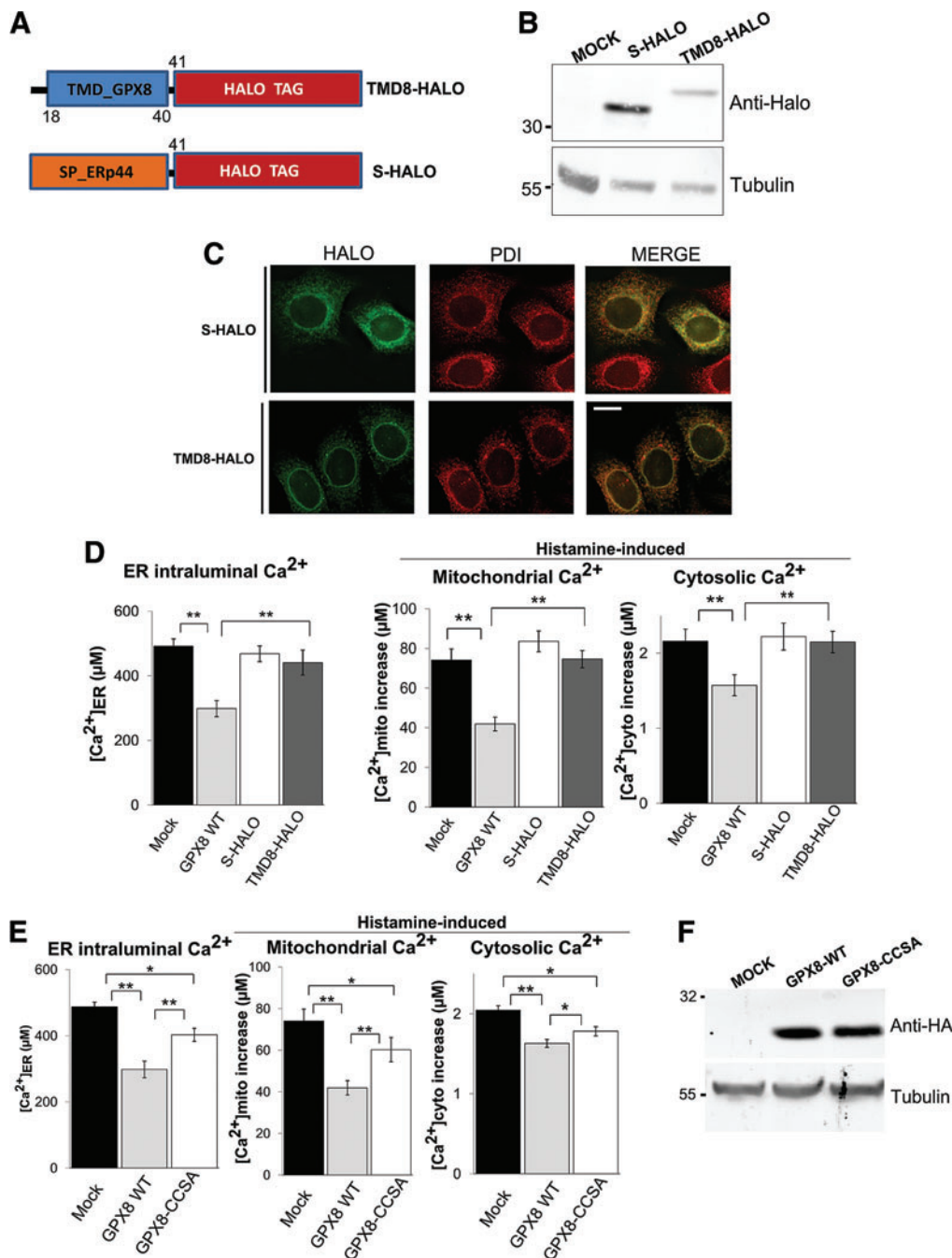


FIG. 6. GPX8 peroxidatic cysteines are involved in Ca^{2+} regulation. (A) Diagram illustrating the constructs used in the following assays (B–D). As previously described (22), S-HALO drives the targeting of the Halo-tag to the ER via the ERp44 cleavable ER signal peptide (SP_ERp44). In TMD8-HALO, the Halotag had been extended with the ER targeting region (1–40) of GPX8, which includes its transmembrane domain (TMD_GPX8). Both proteins contain C-terminal RDEL motifs (not depicted here) for mediating their ER localization. (B) Western blots showing S-HALO and C8-TMD8-HALO protein expression levels. Protein extracts of the corresponding HeLa transfectants were separated by SDS-PAGE and analyzed by Western blotting with the indicated antibodies. (See Supplementary Fig. S12 for uncropped Western blots). (C) Fluorescence microscopy images of fixed transient HeLa transfectants expressing S-HALO and TMD8-HALO. Halo signals were obtained by incubating cells with R110, a fluorescent-specific ligand of the HALO protein, whereas PDI was visualized with an anti-PDI antibody. (Scale bar, 10 μ m) (D) HeLa cells were co-transfected with plasmids encoding S-HALO or TMD8-HALO or the empty parental vector. The $[Ca^{2+}]_{ER}$, mitochondrial, and cytosolic Ca^{2+} responses were monitored as described in the Material and Methods section 36 h after transfection. The data are pooled from ~15 independent experiments and are expressed as the mean \pm SE, $**p < 0.01$. (E) Western blot illustrating the expression of GPX8 WT and GPX8-CCSA (GPX8 with Cys79 and 108 mutated in Ser and Ala, respectively). Numbers on the left indicate the relative molecular weight based on co-migrating pre-stained molecular weight markers. (See Supplementary Fig. S12 for uncropped Western blots.) (F) HeLa cells were co-transfected with plasmids encoding GPX8-CCSA, GPX8-WT, or empty parental vector, as well as organelle-specific aequorin probes. $[Ca^{2+}]_{ER}$, mitochondrial, and cytosolic Ca^{2+} responses were monitored as described in the Materials and Methods section, $n = 25$ independent experiments, $**p < 0.01$ and $*p < 0.05$. To see this illustration in color, the reader is referred to the web version of this article at www.liebertpub.com/ars

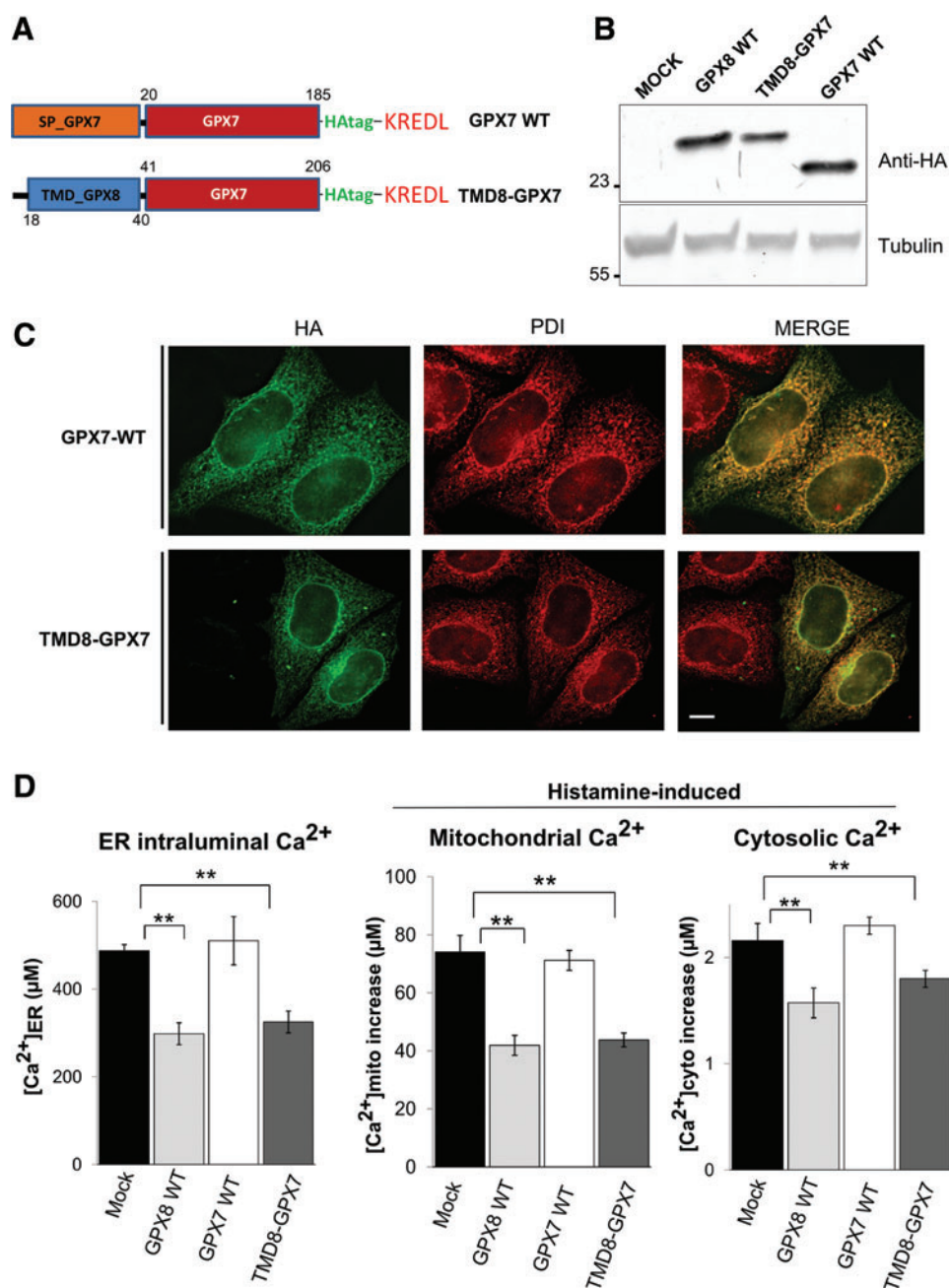


FIG. 7. GPX7 regulates Ca^{2+} dynamics only if fused to the GPX8 transmembrane domain. (A) Diagram illustrating the main differences between GPX7-WT and the TMD8-GPX7 variants. In TMD8-GPX7, the regular and cleavable signal peptide of GPX7 (SP_GPX7) has been substituted by the GPX8 ER targeting region (1–40), which includes the TMD (TMD_GPX8). (B) Western blot analyses confirming the expression of GPX8-WT, GPX7-WT, and TMD8-GPX7. Numbers on the left indicate the relative molecular weight based on co-migrating pre-stained molecular weight markers. (See Supplementary Fig. S13 for uncropped Western blots). (C) Immunofluorescence staining performed on fixed HeLa cells transiently expressing GPX7-WT or TMD8-GPX7 as indicated. Cells were double stained with anti-HA and anti-PDI antibodies (Scale bar, 10 μ m). (D) HeLa cells were co-transfected with plasmids encoding GPX8-WT, GPX7-WT, TMD8-GPX7, or the corresponding empty parental vector, as well as organelle-specific aequorin probes. $[Ca^{2+}]_{ER}$, mitochondrial, and cytosolic Ca^{2+} responses were monitored as described in the Materials and Methods section. The data are pooled from ~ 15 independent experiments and are expressed as the mean \pm SE, $**p < 0.01$. To see this illustration in color, the reader is referred to the web version of this article at www.liebertpub.com/ars

A1978, respectively; Sigma Aldrich); and anti-Calnexin and anti-GRP94 (SPA-860 and SPA-851, respectively; Enzo Life Sciences). Fluorescent goat anti-mouse and anti-rabbit IgG (H + L) Alexa Fluor conjugated 647, 546, and 488 were from Invitrogen Molecular Probes (Eugene, OR).

Culture media were from Invitrogen Life Technologies. HeLa cell lines were purchased from ATCC. Tissue culture, transfection, and silencing were performed as previously described (2). All the other reagents were from Sigma-Aldrich (St. Louis, MO).

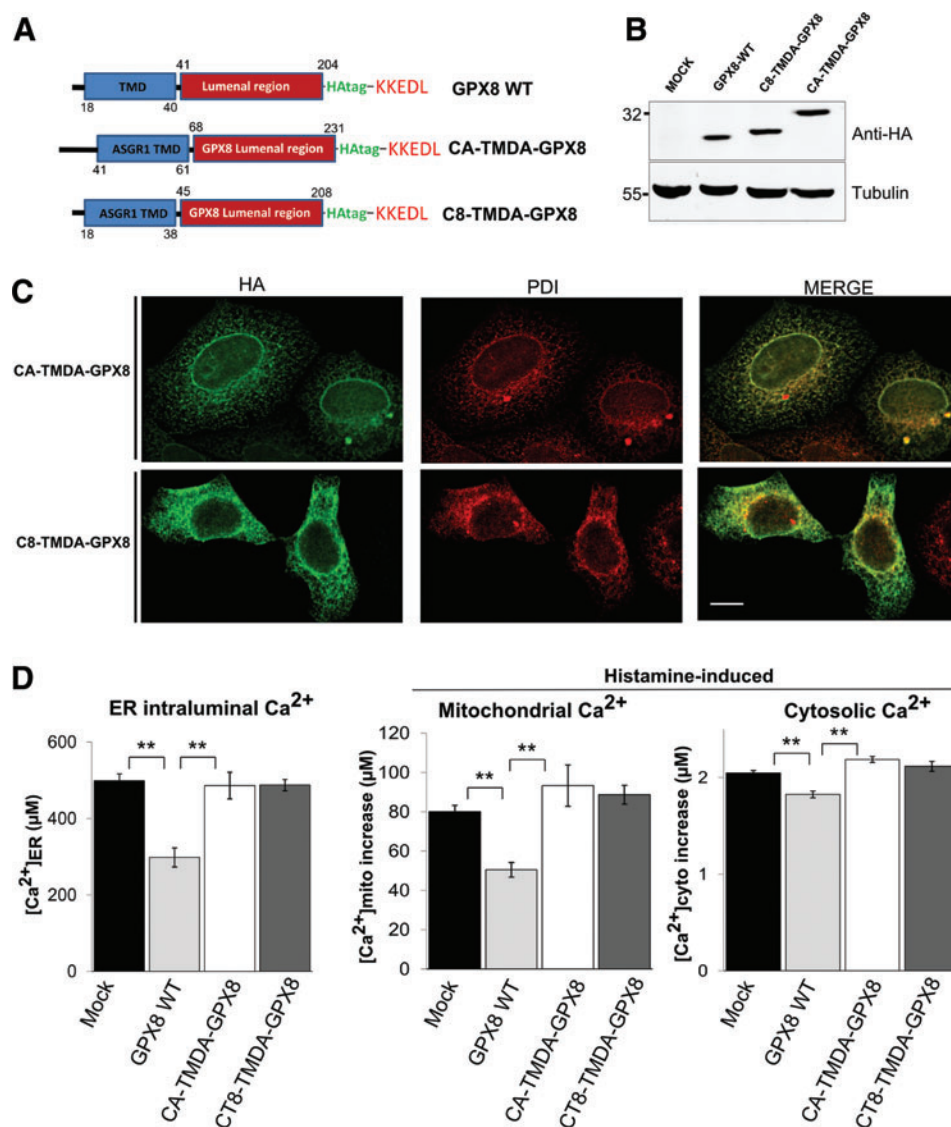


FIG. 8. The N-terminal hydrophobic stretch is specifically required for conferring Ca^{2+} regulatory properties to GPX8. (A) Similar to the other figures, the diagram summarizes the main features of the GPX8 variants used. In CA-TMDA-GPX8, the first 40 amino acids of GPX8, which include its TMD, were replaced by the N-terminal region (residues 1–61) of the ASGR1 receptor, which is also a type II transmembrane protein with its TMD (TMD_ASGR1) spanning from residues 41 to 61. In C8-TMDA-GPX8, the cytosolic N-terminal tip of GPX8 has been conserved whereas only the TMD of GPX8 has been substituted with the one of ASGR1. The Western blots in (B) show the expression levels of GPX8-WT, CA-TMDA-GPX8, and C8-TMDA-GPX8. (See Supplementary Fig. S14 for uncropped Western blots.) (C) Fixed HeLa cells transiently expressing CA-TMDA-GPX8 (upper panels) and C8-TMDA-GPX8 (lower panels) were double stained with anti-HA and anti-PDI antibodies (Scale bar, 10 μ m). (D) HeLa cells were co-transfected with plasmids encoding GPX8-WT, CA-TMDA-GPX8, C8-TMDA-GPX8, and the corresponding empty parental vector, as well as organelle-specific aequorin probes. $[Ca^{2+}]_{ER}$, mitochondrial, and cytosolic Ca^{2+} responses were monitored as described in the Materials and Methods section. The data are pooled from ~ 15 independent experiments and are expressed as the means \pm SE, ** $p < 0.01$. To see this illustration in color, the reader is referred to the web version of this article at www.liebertpub.com/ars

Subcellular fractionation

After homogenization of the cells, crude mitochondrial and microsomal fractions were separated by classical differential centrifugation. Subsequently, the crude mitochondrial fraction was resuspended in isolation buffer (250 mM mannitol, 5 mM HEPES, 0.5 mM EGTA, pH 7.4) and further separated on a 30% Percoll gradient to obtain low-density (denoted as MAM) and high-density (denoted as pure mitochondria, Mito Pure) fractions as described in Ref. (46).

Aliquots of the fractions were collected and analyzed by Western blot after SDS-PAGE was performed on an equal quantity of proteins.

Protein extraction, electrophoresis, and Western blot

Cells were trypsinized, washed in PBS, and lysed in RIPA buffer (150 mM NaCl, 1% NP-40, 0.1% SDS, 50 mM Tris-HCl pH 8.0) that was supplemented with NEM 10 mM and

protease inhibitors cocktail (Roche). After centrifugation at 14,000g at 4°C, proteins were separated by reducing SDS-PAGE on gradient 4–12% Bis-Tris polyacrylamide precast gel gradient (Life Technologies) or 15% homemade Tris-glycine SDS-PAGE.

After electrotransfer onto nitrocellulose membrane and probing with the desired antibodies, the proteins were visualized with FLA-900 Starion (when fluorescent secondary antibodies have been used) or electrochemiluminescence (ECL prime, GE Healthcare) when using HRP-coupled secondary antibodies.

Calcium measurements

Cells were plated onto 13 × 13 mm coverslips at a density of 5×10^5 cells/coverslip; then, they were co-transfected with organelle-specific aequorin-based probes and GPX8 or its mutants. The probes employed (cytAEQ, mtAEQ, and erAEQ) are chimeric aequorins that are targeted to the cytosol, mitochondria, and ER, respectively (4).

For the experiments with cytAEQ and mtAEQ, cells were incubated with 5 μ M coelenterazine for 1–2 h in DMEM that was supplemented with 1% fetal calf bovine (FCS). Then, the coverslip with transfected cells was placed in a perfused chamber with a thermostat, located in close proximity of a low-noise photomultiplier, with a built-in amplifier-discriminator.

To reconstitute the erAEQ with high efficiency, the luminal $[Ca^{2+}]$ of the stores first had to be reduced. This was achieved by incubating the cells for 45 min at 4°C in Krebs Ringer Buffer (KRB), which was supplemented with 5 μ M coelenterazine, the Ca^{2+} ionophore ionomycin, and 600 μ M EGTA. After 45 min, cells were extensively washed with KRB, supplemented with 2% bovine serum albumin, and finally transferred to the perfusion chamber. All aequorin measurements were carried out in KRB that was supplemented with either 1 mM $CaCl_2$ (cytAEQ and mtAEQ) or 100 μ M EGTA (erAEQ).

Agonists (100 μ M histamine, 1 μ M Bradykinin) were perfused to the same medium to induce IP₃-dependent Ca^{2+} release from ER, generating a rapid rise in cytosolic and mitochondrial $[Ca^{2+}]$ followed by a gradual decline to a lower plateau, as reported in Supplementary Figure S1. The experiments were terminated by lysing cells with 100 μ M Triton in a hypotonic Ca^{2+} -containing solution (10 mM $CaCl_2$ in H₂O), thus discharging the remaining aequorin pool. The output of the discriminator was captured by a Thorn-EMI photon counting board and stored in an IBM-compatible computer for further analyses. The aequorin luminescence data were calibrated off-line into $[Ca^{2+}]$ values, using a computer algorithm based on the Ca^{2+} response curve of wt or mutated aequorin (4). Statistical data are expressed as the mean of agonist-dependent ER-, mitochondrial- and cytosolic Ca^{2+} response \pm standard error (SE).

To measure SERCA2b activity, the Ca^{2+} uptake rate was analyzed by the OriginLab analysis program, measured from the first derivative considering the first 30 s of measurements from Ca^{2+} addition in erAEQ-based experiments. The data obtained are expressed as mean of ER Ca^{2+} accumulation rate per second \pm SE (μ M/s). For measurements of ER Ca^{2+} leak rate, HeLa cells were co-transfected with erAEQ and the indicated constructs or siRNA. Thirty-six hours after transfection, depletion of Ca^{2+} stores and AEQ reconstitution was performed. The coverslip with the cells was transferred to the

luminometer and perfused with KRB/ Ca^{2+} until the steady-state $[Ca^{2+}]_{ER}$ was reached. The ER was refilled by exposing cells to extracellular $[Ca^{2+}]$ ranging from 0.1 to 1 mM, to obtain different levels of steady-state $[Ca^{2+}]_{ER}$. Cells were then treated with the SERCA inhibitor tBHQ (30 μ M), and the consequent decrease of $[Ca^{2+}]_{ER}$, due to passive efflux, was then analyzed. The maximal rates of Ca^{2+} release at different $[Ca^{2+}]_{ER}$ values were calculated (measured from the first derivative considering 15 s after tBHQ addition). To minimize the effects of the $[Ca^{2+}]_{ER}$ on passive efflux, cells in the 250–350 μ M range of plateau values were compared. The rate of decline of $[Ca^{2+}]_{ER}$ must reflect the rate of ER Ca^{2+} extrusion, shown as response mean \pm SE (μ M/s) for each of the experimental conditions.

Plasmid construction

For generating the plasmid overexpressing an HA-tagged version of the wild-type form of GPX8 (GPX8 WT) and the catalytically inactive GPx8 (GPx8-C79S), GPx8-HA sequences on the pRK7 vector (pKEHS768; a kind gift of L. Ruddock, Oulu, Finland) and on the pcDNA 3.0 vector (kindly provided by C. Appenzeller-Herzog, Basel, Switzerland), respectively, were excised and subcloned into pcDNA3.1 by using *Bam*HI and *Hind*III. The plasmid expressing GPX8-C79S was used as a template for site-directed mutagenesis by PCR of C108 in A to generate the plasmid GPX8-CCSA. To generate the transmembrane-less form of GPX8 (S-GPX8), the sequence encoding for the HA-tagged luminal part of GPX8 was amplified by PCR by using the following primers: GGCGCgcatgctgctgaaAAACCTAAAA TCAACAGC; CCGGggtatccTCATAGATCC TCTTTCTT tgcg; and the plasmid pKEHS768 as templates. The PCR product was digested with *Sgf*I and *Bam*HI restriction enzymes and cloned in frame with the encoding sequence of the signal peptide of ERp44 into a pcDNA3.1 vector. The S-Halo encoding plasmid has been previously described (22).

For generating TMD8-Halo, the primers ggtagctctagacc accATGGAGCCTC and cctctgcatgctgctTTTAGGTTTgaggaa were used for amplifying by PCR the residues 1–43 of GPX8 by using the plasmid pKEHS768 as a template. The PCR product and the S-Halo plasmid were digested with the *Sgf*I and *Xba*I enzymes and ligated for completing the construction. HA-tag and the KREDL motif naturally found at the C-terminus of GPX7 were added through PCR to generate the plasmid overexpressing GPX7.

This plasmid was used as a template for amplifying by PCR the sequence encoding for the matured form of GPX7. The PCR product was substituted for the HALO tag in the plasmid C8-TMD8-Halo for generating the C8-TMD8-GPX7 encoding plasmid. GPX8 small interfering RNA was purchased from Ambion (Life Technologies).

For obtaining the plasmid encoding for GPX8 fused to the TMD of ASGR1 (CA-TMDA-GPX8), the sequence encoding for the 67 first N-terminus residues of ASGR1 was amplified by PCR. The PCR product was substituted for the signal peptide of ERp44 present in the S-GPX8 plasmid. The plasmid CA-TMDA-GPX8 was used as a template for PCR generating the plasmid C8-TMDA-GPX8. Primer sequences are available through request. All constructs were validated by sequencing (GATC Biotech, Germany). Silencing was performed by using RNAiMAX (Invitrogen, Carlsbad, CA) based on the manufacturer's instructions.

Fluorescence microscopy experiments

Glass-plated cells were transfected with the plasmid of interest and grown for 48 h. Cells were then fixed by using 4% paraformaldehyde, permeabilized with 0.2% Triton X-100, and finally incubated with the suitable antibodies (1:100 and 1:200 dilutions for the primary and secondary, respectively). After mounting, images were acquired and analyzed by using the DeltaVision RT Deconvolution System (GE Healthcare).

Measurements of ER Ca^{2+} dynamics with D1ER

Intraluminal Ca^{2+} dynamics were measured by using single-cell Ca^{2+} imaging with the Ca^{2+} -sensitive FRET (fluorescence resonance energy transfer)-based chameleon protein D1ER (26). HeLa cells were co-transfected with D1ER and GPX8 WT. After 36 h, coverslips were placed in 1 ml of KRB/EGTA Ca^{2+} free and TBHQ 20 μM for 15 min. After washing, the coverslips were maintained in KBR Ca^{2+} free and images were captured with METAFLUOR 7.0 Software (Universal Imaging) at $\lambda_{\text{excitation}} = 430 \text{ nm}$ and $\lambda_{\text{emission}} = 470$ and 535 nm every 1 s by using a Zeiss Axiovert 200M inverted microscope equipped with a C-Apochromat 40 \times /1.2 W CORR objective and a cooled CCD camera (Photometrics). Cyan fluorescent protein (CFP) emission and yellow fluorescent protein FRET emission were alternately collected at 470 and 535 nm, respectively. The FRET signal was normalized to the CFP emission intensity, and changes in ER Ca^{2+} were expressed as the ratio of the emissions at 535 and 470 nm. Cells were perfused with KRB Ca^{2+} free at the beginning of the experiment and the baseline of the FRET ratio was measured, which corresponds to ER-depleted Ca^{2+} level. Then, Ca^{2+} (1 mM) was added to the perfusion, thus stimulating ER Ca^{2+} refilling.

Fura-2/AM measurements

The cytosolic-free Ca^{2+} concentration ($[\text{Ca}^{2+}]_c$) was evaluated by using the fluorescent Ca^{2+} indicator Fura-2 acetoxymethyl ester (Fura-2/AM; Molecular Probes). Briefly, cells were incubated in medium that was supplemented with 2.5 μM Fura-2/AM for 30 min, washed with KRB buffer to remove the extracellular probe, supplied with preheated KRB buffer (supplemented with 1 mM CaCl_2), and placed in a thermostated (37°C) incubation chamber on the stage of an inverted fluorescence microscope (Zeiss Axiovert 200). Dynamic video imaging was performed by using the Metafluor software (Universal Imaging Corporation).

Fluorescence was measured every 100 ms with the excitation wavelength alternating between 340 and 380 nm and the emission fluorescence being recorded at 510 nm. At the end of the experiment, a region free of cells was selected, and one averaged background frame was collected at each excitation wavelength for background correction.

The $[\text{Ca}^{2+}]_c$ was calculated by the ratio method by using the equation: $[\text{Ca}^{2+}]_c = \text{Kd} (\text{R} - \text{Rmin}) / (\text{R} - \text{Rmax}) \times \text{Sf2} / \text{Sf1}$, where Kd is the dissociation constant of Fura-2/AM for (Ca^{2+}) taken as 240 nM at 37°C, R is the ratio of fluorescence for Fura-2/AM at the two excitation wavelengths, F340/F380, Rmax is the ratio of fluorescence in the presence of excess of Ca^{2+} obtained by lysing the cells with 10 μM ionomycin (Sigma Aldrich), Rmin is the ratio of fluorescence in the presence of minimal Ca^{2+} obtained by lysing the cells and then

chelating all the Ca^{2+} with 0.5 M EGTA, Sf2 is the fluorescence of the Ca^{2+} -free form of Fura-2/AM at 380 nm excitation wavelength, and Sf1 is the fluorescence of the Ca^{2+} -bound form of Fura-2/AM at 380 nm excitation wavelength.

Mitochondrial Ca^{2+} concentration measurements with 2mt-GCaMP6m

To test resting mitochondrial Ca^{2+} concentrations with high sensitivity, we used the Ca^{2+} probe based on the last-generation GCaMP probe targeted to the mitochondrial matrix (7). We chose the GCaMP6m version, because it had the highest Ca^{2+} affinity. To measure the signal independent of variations in basal fluorescence intensity due to the variable expression levels of the probe, we took advantage of the isosbestic point in the GCaMP6m the excitation spectrum; exciting GCaMP6m at 410 nm led to fluorescence emission that was not Ca^{2+} dependent. As a consequence, the ratio between the excitation wavelengths of 474 and 410 nm was proportional to the Ca^{2+} concentration and independent of probe expression levels. Cells were imaged with an IX-81 automated epifluorescence microscope (Olympus) that was equipped with a 40 \times oil immersion objective and an ORCA-R2 charge-coupled device camera (Hamamatsu Photonics).

Acknowledgments

The authors thank members of the P.P., R.S., and van Anken laboratories for helpful suggestions and discussions; Claudio Fagioli and Roberta Colzani for precious technical and secretarial assistance, respectively. They are extremely grateful to Drs. Christian Appenzeller-Herzog, Lloyd Rud-dock, and Lei Wang for their generous gifts of plasmids and suggestions. They thank Dr. Julia Birk, Dr. Darius Moradpour, and Dr. Ineke Braakman for providing useful reagents. E.D.Y. and R.S. thank Sara Alameddine, Andrea Giordano, Lucilla Sciaqua, and Paolo Tesaro for help rendered during plasmid constructions. P.P. is grateful to Camilla degli Scrovegni for her continuous support.

Part of this work was carried out in the Advanced Light and Electron Microscopy BioImaging Center (ALEMBIC) of San Raffaele Scientific Institute and Vita-Salute University.

This work was supported in part by grants from AIRC (IG14559, IG18824), Fondazione Cariplo (2015-0591), Fondazione Banca del Monte di Lombardia, Ministero della Salute (PE-2011-02352286), and Telethon (GGP15059) to R.S., E.D.Y. was recipient of a Marie Curie Fellowship through the INVEST-COFUND program (PCOFUND-GA-2010-267264 INVEST).

This work was also supported by the local funds from the University of Ferrara to A.R. and P.P. and grants from the Italian Ministry of Health (GR-2011-02346964), the Italian Cystic Fibrosis Foundation (FFC #20/2015) to A.R., and by grants from the Italian Association for Cancer Research (AIRC, IG-18624), Telethon (GGP15219B), the Italian Cystic Fibrosis Foundation (FFC #19/2014), the Italian Ministry of Education, University and Research (COFIN: 20129JLHSY_002, FIRB: RBAP11FXBC_002, Futuro in Ricerca: RBFR10EGVP_001), and the Italian Ministry of Health to P.P.

Author Disclosure Statement

No competing financial interests exist.

References

1. Anelli T, Bergamelli L, Margittai E, Rimessi A, Fagioli C, Malgaroli A, Pinton P, Ripamonti M, Rizzuto R, and Sitia R. Ero1 α regulates Ca²⁺ fluxes at the endoplasmic reticulum-mitochondria interface (MAM). *Antioxid Redox Signal* 16: 1077–1087, 2012.
2. Anelli T, Ceppi S, Bergamelli L, Cortini M, Masciarelli S, Valetti C, and Sitia R. Sequential steps and checkpoints in the early exocytic compartment during secretory IgM biogenesis. *EMBO J* 26: 4177–4188, 2007.
3. Appenzeller-Herzog C and Simmen T. ER-luminal thiol/selenol-mediated regulation of Ca²⁺ signalling. *Biochem Soc Trans* 44: 452–459, 2016.
- 3b. Ashwell G and Harford J. Carbohydrate-specific receptors of the liver. *Annu Rev Biochem* 51: 531–554, 1982.
4. Bonora M, Giorgi C, Bononi A, Marchi S, Patergnani S, Rimessi A, Rizzuto R, and Pinton P. Subcellular calcium measurements in mammalian cells using jellyfish photo-protein aequorin-based probes. *Nat Protoc* 8: 2105–2118, 2013.
5. Bosello-Travain V, Forman HJ, Roveri A, Toppo S, Ursini F, Venerando R, Warnecke C, Zaccarin M, and Maiorino M. Glutathione peroxidase 8 is transcriptionally regulated by HIF α and modulates growth factor signaling in HeLa cells. *Free Radic Biol Med* 81: 58–68, 2015.
6. Brigelius-Flohé R and Maiorino M. Glutathione peroxidases. *Biochim Biophys Acta* 1830: 3289–3303, 2013.
7. Chen T-W, Wardill TJ, Sun Y, Pulver SR, Renninger SL, Baohan A, Schreiter ER, Kerr RA, Orger MB, Jayaraman V, Looger LL, Svoboda K, and Kim DS. Ultrasensitive fluorescent proteins for imaging neuronal activity. *Nature* 499: 295–300, 2013.
8. Csala M, Kereszturi E, Mandl J, and Bánhegyi G. The endoplasmic reticulum as the extracellular space inside the cell: Role in protein folding and glycosylation. *Antioxid Redox Signal* 16: 1100, 2012.
9. Delaunay-Moisan A and Appenzeller-Herzog C. The antioxidant machinery of the endoplasmic reticulum: protection and signaling. *Free Radic Biol Med* 83: 341–351, 2015.
10. This reference has been deleted.
11. García-Pérez C, Hajnóczky G, and Csordás G. Physical coupling supports the local Ca²⁺ transfer between sarcoplasmic reticulum subdomains and the mitochondria in heart muscle. *J Biol Chem* 283: 32771–32780, 2008.
12. Gilady SY, Bui M, Lynes EM, Benson MD, Watts R, Vance JE, and Simmen T. Ero1 α requires oxidizing and normoxic conditions to localize to the mitochondria-associated membrane (MAM). *Cell Stress Chaperones* 15: 619–629, 2010.
13. Giorgi C, Missiroli S, Patergnani S, Duszynski J, Wieckowski MR, and Pinton P. Mitochondria-associated membranes: composition, molecular mechanisms, and physiopathological implications. *Antioxid Redox Signal* 22: 995–1019, 2015.
14. Grupe M, Myers G, Penner R, and Fleig A. Activation of store-operated I(CRAC) by hydrogen peroxide. *Cell Calcium* 48: 1–9, 2010.
15. Hajnóczky G, Csordás G, Madesh M, and Pacher P. Control of apoptosis by IP3 and ryanodine receptor driven calcium signals. *Cell Calcium* 28: 349–363, 2000.
16. Holmström KM and Finkel T. Cellular mechanisms and physiological consequences of redox-dependent signalling. *Nat Rev Mol Cell Biol* 15: 411–421, 2014.
17. Horner SM, Liu HM, Park HS, Briley J, and Gale M. Mitochondrial-associated endoplasmic reticulum membranes (MAM) form innate immune synapses and are targeted by hepatitis C virus. *Proc Natl Acad Sci* 108: 14590–14595, 2011.
18. Kakihana T, Nagata K, and Sitia R. Peroxides and peroxidases in the endoplasmic reticulum: integrating redox homeostasis and oxidative folding. *Antioxid Redox Signal* 16: 763–771, 2012.
19. Los GV, Encell LP, McDougall MG, Hartzell DD, Karsassina N, Zimprich C, Wood MG, Learish R, Ohana RF, Urh M, Simpson D, Mendez J, Zimmerman K, Otto P, Vidugiris G, Zhu J, Darzins A, Klaubert DH, Bulleit RF, and Wood KV. HaloTag: a novel protein labeling technology for cell imaging and protein analysis. *ACS Chem Biol* 3: 373–382, 2008.
20. Lynes EM and Simmen T. Urban planning of the endoplasmic reticulum (ER): how diverse mechanisms segregate the many functions of the ER. *Biochim Biophys Acta* 1813: 1893–1905, 2011.
21. Morikawa K, Gouttenoire J, Hernandez C, Dao Thi VL, Tran HTL, Lange CM, Dill MT, Heim MH, Donzé O, Penin F, Quadroni M, and Moradpour D. Quantitative proteomics identifies the membrane-associated peroxidase GPx8 as a cellular substrate of the hepatitis C virus NS3-4A protease. *Hepatology* 59: 423–433, 2014.
22. Mossuto MF, Sannino S, Mazza D, Fagioli C, Vitale M, Yoboue ED, Sitia R, and Anelli T. A dynamic study of protein secretion and aggregation in the secretory pathway. *PLoS One* 9: e108496, 2014.
23. Nguyen VD, Saaranen MJ, Karala A-R, Lappi A-K, Wang L, Raykhel IB, Alanen HI, Salo KEH, Wang C, and Rudnick LW. Two endoplasmic reticulum PDI peroxidases increase the efficiency of the use of peroxide during disulfide bond formation. *J Mol Biol* 406: 503–515, 2011.
24. Nunes P and Demareux N. Redox regulation of store-operated Ca²⁺ entry. *Antioxid Redox Signal* 21: 915–932, 2013.
25. Oakes SA, Scorrano L, Opferman JT, Bassik MC, Nishino M, Pozzan T, and Korsmeyer SJ. Proapoptotic BAX and BAK regulate the type 1 inositol trisphosphate receptor and calcium leak from the endoplasmic reticulum. *Proc Natl Acad Sci U S A* 102: 105–110, 2005.
26. Palmer AE, Jin C, Reed JC, and Tsien RY. Bcl-2-mediated alterations in endoplasmic reticulum Ca²⁺ analyzed with an improved genetically encoded fluorescent sensor. *Proc Natl Acad Sci U S A* 101: 17404–17409, 2004.
27. Patergnani S, Suski JM, Agnoletto C, Bononi A, Bonora M, De Marchi E, Giorgi C, Marchi S, Missiroli S, Poletti F, Rimessi A, Duszynski J, Wieckowski MR, and Pinton P. Calcium signaling around mitochondria associated membranes (MAMs). *Cell Commun Signal* 9: 19, 2011.
28. Phillips MJ and Voeltz GK. Structure and function of ER membrane contact sites with other organelles. *Nat Rev Mol Cell Biol* 17: 69–82, 2015.
29. Ramming T and Appenzeller-Herzog C. Destroy and exploit: catalyzed removal of hydroperoxides from the endoplasmic reticulum. *Int J Cell Biol* 2013: e180906, 2013.
30. Ramming T, Hansen HG, Nagata K, Ellgaard L, and Appenzeller-Herzog C. GPx8 peroxidase prevents leakage of H₂O₂ from the endoplasmic reticulum. *Free Radic Biol Med* 70: 106–116, 2014.
31. Ramming T, Okumura M, Kanemura S, Baday S, Birk J, Moes S, Spiess M, Jenö P, Bernèche S, Inaba K, and Appenzeller-Herzog C. A PDI-catalyzed thiol-disulfide

- switch regulates the production of hydrogen peroxide by human Ero1. *Free Radic Biol Med* 83: 361–372, 2015.
32. Raturi A and Simmen T. Where the endoplasmic reticulum and the mitochondrion tie the knot: the mitochondria-associated membrane (MAM). *Biochim Biophys Acta* 1833: 213–224, 2013.
 33. Raykhel I, Alanen H, Salo K, Jurvansuu J, Nguyen VD, Latva-Ranta M, and Ruddock L. A molecular specificity code for the three mammalian KDEL receptors. *J Cell Biol* 179: 1193–1204, 2007.
 34. Rigoulet M, Yoboue ED, and Devin A. Mitochondrial ROS generation and its regulation: mechanisms involved in H(2)O(2) signaling. *Antioxid Redox Signal* 14: 459–468, 2011.
 35. Rimessi A, Giorgi C, Pinton P, and Rizzuto R. The versatility of mitochondrial calcium signals: from stimulation of cell metabolism to induction of cell death. *Biochim Biophys Acta* 1777: 808–816, 2008.
 36. Ronzoni R, Anelli T, Brunati M, Cortini M, Fagioli C, and Sitia R. Pathogenesis of ER storage disorders: modulating Russell body biogenesis by altering proximal and distal quality control. *Traffic* 11: 947–957, 2010.
 37. Schäuble N, Lang S, Jung M, Cappel S, Schorr S, Ulucan Ö, Linxweiler J, Dudek J, Blum R, Helms V, Paton AW, Paton JC, Cavalié A, and Zimmermann R. BiP-mediated closing of the Sec61 channel limits Ca²⁺ leakage from the ER. *EMBO J* 31: 3282–3296, 2012.
 38. Spiess M and Lodish HF. An internal signal sequence: the asialoglycoprotein receptor membrane anchor. *Cell* 44: 177–185, 1986.
 39. Toppo S, Vanin S, Bosello V, and Tosatto SCE. Evolutionary and structural insights into the multifaceted glutathione peroxidase (Gpx) superfamily. *Antioxid Redox Signal* 10: 1501–1514, 2008.
 40. Utomo A, Jiang X, Furuta S, Yun J, Levin DS, Wang Y-CJ, Desai KV, Green JE, Chen P-L, and Lee W-H. Identification of a novel putative non-selenocysteine containing phospholipid hydroperoxide glutathione peroxidase (NPGPx) essential for alleviating oxidative stress generated from polyunsaturated fatty acids in breast cancer cells. *J Biol Chem* 279: 43522–43529, 2004.
 41. Van Coppenolle F, Vanden Abeele F, Slomianny C, Flourakis M, Hesketh J, Dewailly E, and Prevarskaya N. Ribosome-translocon complex mediates calcium leakage from endoplasmic reticulum stores. *J Cell Sci* 117: 4135–4142, 2004.
 42. Vance JE. Phospholipid synthesis in a membrane fraction associated with mitochondria. *J Biol Chem* 265: 7248–7256, 1990.
 43. Vance JE. MAM (mitochondria-associated membranes) in mammalian cells: lipids and beyond. *Biochim Biophys Acta* 1841: 595–609, 2014.
 44. Vandecaetsbeek I, Vangheluwe P, Raeymaekers L, Wuytack F, and Vanoevelen J. The Ca²⁺ pumps of the endoplasmic reticulum and Golgi apparatus. *Cold Spring Harb Perspect Biol* 3: a004184, 2011.
 45. Wang L, Zhang L, Niu Y, Sitia R, and Wang C. Glutathione peroxidase 7 utilizes hydrogen peroxide generated by Ero1 α to promote oxidative protein folding. *Antioxid Redox Signal* 20: 545–556, 2013.
 46. Wieckowski MR, Giorgi C, Lebedzinska M, Duszynski J, and Pinton P. Isolation of mitochondria-associated membranes and mitochondria from animal tissues and cells. *Nat Protoc* 4: 1582–1590, 2009.

Address correspondence to:

Dr. Roberto Sitia
Protein Transport and Secretion Unit
Division of Genetics and Cell Biology
IRCCS Ospedale San Raffaele and
Università Vita-Salute San Raffaele
Via Olgettina 58
20132 Milan
Italy

E-mail: sitia.roberto@hsr.it

Date of first submission to ARS Central, August 16, 2016; date of final revised submission, January 21, 2017; date of acceptance, January 26, 2017.

Abbreviations Used

ER = endoplasmic reticulum
Ero1 = endoplasmic reticulum oxidoreductin 1
GPX = glutathione peroxidase
IP3 = inositol 1,4,5-trisphosphate
IP3R = inositol 1,4,5-trisphosphate receptor
KRB = Krebs ringer buffer
MAM = mitochondria-associated membranes
MCU = mitochondrial calcium uniporter
PDI = protein disulfide isomerase
SERCA = sarcoendoplasmic reticulum calcium ATPase
tBHQ = 2,5-di-(terbutyl)-1,4-benzohydroquinone
TMD = transmembrane domain
TMD8 = transmembrane domain of GPX8
TOM20 = mitochondrial import receptor subunit
TOM20 homolog